



Estimation of the state and parameters in ice sheet model using an ensemble Kalman filter and Observing System Simulation Experiments

Youngmin Choi¹, Alek Petty¹, Denis Felikson², and Jonathan Poterjoy³

Correspondence: Youngmin Choi (yochoi@umd.edu)

Abstract. Better constraining the current and future evolution of Earth's ice sheets using physical process models is essential for improving our understanding of future sea level rise. Data assimilation is a method that combines models with observations to improve current estimates of model states and parameters, leveraging the information and uncertainties inherent in both models and observations. In this study, we present an ensemble Kalman filter-based data assimilation (DA) framework for ice sheet modeling, aiming to better constrain the model state and key parameters from a single semi-idealized glacier domain. Through a synthetic twin experiment, we show that the ensemble DA method effectively recovers basal conditions and the model state after a few assimilation cycles. Assimilating more observations improves the accuracy of these estimates, thereby improving the model's projection capabilities. We also utilize Observing System Simulation Experiments (OSSEs) to explore the capabilities of the ensemble DA framework to assimilate different types of data and to quantify their impact on the model state and parameter estimation. In our experiments, we assimilate land ice elevation data simulated based on The Ice, Cloud, and Land Elevation Satellite-2 (ICESat-2) products. These experiments are crucial for identifying observations with the largest impact on state and parameter estimates. Our assimilation results are highly sensitive to design choices for observation networks, such as spatial resolutions and prescribed uncertainties. The ensemble DA framework, capable of assimilating multi-temporal observations, shows promising results for real glacier applications through a continental ice sheet model. Additionally, this framework provides a flexible infrastructure for performing OSSEs aimed at testing various observational settings for future missions, as it requires less numerical development than variational methods.

1 Introduction

The combined contribution of the Greenland Ice Sheet (GrIS) and the Antarctic Ice Sheet (AIS) to global sea level is one of the most significant sources of uncertainty in projections of sea-level rise for the coming century (Intergovernmental Panel on Climate Change (IPCC), 2023). In recent years, numerical ice sheet models have significantly advanced through improved ice flow physics, enhanced spatial resolution, and their ability to simulate moving boundaries (Nowicki and Seroussi, 2018). Despite these advancements, projections of mass change for both the AIS and GrIS, and consequently their contributions to

¹Earth System Science Interdisciplinary Center, University of Maryland, College Park, MD, USA

²NASA Goddard Space Flight Center, Greenbelt, MD, USA

³Department of Atmospheric & Oceanic Science, University of Maryland, College Park, MD, USA



25



sea-level rise over the coming century, exhibit significant spread, primarily due to uncertainty in key model parameters and model initialization (Nowicki et al., 2016; Seroussi et al., 2020; Goelzer et al., 2020).

Data assimilation (DA) is a method of combining information from models with observations to improve the accuracy of the model state variables and/or specific model parameters. Currently, most ice sheet models use variational data assimilation methods to constrain basal conditions (e.g., friction coefficient) and estimate the present state of the ice sheet using surface observations (e.g., surface velocity) (Gillet-Chaulet, 2020). However, these approaches generally rely on a single instance of observations to perform time-independent inversions of model parameters. This method captures a specific state of the ice sheet at a particular time (Morlighem et al., 2013; Gillet-Chaulet et al., 2012), but it risks introducing nonphysical artifacts from the model's initial state, potentially propagating artifacts into transient simulations rather than capturing actual trends of changes in ice dynamics (Seroussi et al., 2011; Goldberg et al., 2015). Such artifacts in initial conditions could affect model simulations over centuries to millennia due to the slow response time of ice sheets (Seroussi et al., 2019). Alternatively, data assimilation techniques that leverage time-varying surface observations have been developed to more accurately constrain ice flow over longer periods. The development of computational techniques such as automatic differentiation (Goldberg and Heimbach, 2013) has enabled the assimilation of more observations into transient model simulations, thereby capturing the model evolution during the assimilation period. While this method has been applied in regional modeling studies (Larour et al., 2014; Goldberg et al., 2015; Choi et al., 2023), scaling time-varying data assimilation approaches for simulations covering entire ice sheets remains challenging due to the complexities involved in developing a time-dependent adjoint model and the substantial memory requirements of automatic differentiation (Choi et al., 2023). Furthermore, variational methods do not explicitly compute the uncertainty coming from the model state and parameters (Carrassi et al., 2018).

Ensemble data assimilation methods that employ the Ensemble Kalman filter (EnKF) have been effective for assimilating diverse observations into complex, large-scale and non-linear geophysical models (Carrassi et al., 2018). The underlying principle of the Kalman filter involves the sequential assimilation of data to estimate state variables for numerical models. This is achieved by iteratively adjusting the model state to better represent the unknown 'true' state of the system (Carrassi et al., 2018) based on noisy observations. The assimilation based on the EnKF is carried out across an ensemble of model runs, each representing plausible system states. As new observations are incorporated within the assimilation period, the ensemble mean presents an increasingly more accurate estimate of the model state. When the model state is updated at each assimilation time, the model parameters can also be updated alongside state variables to reflect past and present observations (Iglesias et al., 2013). Unlike time-independent inversions relying on snapshot of observations from a single time, this framework enables the use of a time series of observations to provide an improved estimate of the model state and parameters. In addition, EnKFs, similar to the classic Kalman filter, provide a direct estimate of uncertainty in model state and parameter estimates, which is represented heuristically through the sample error covariance.

While ensemble DA is less commonly employed in ice sheet modeling compared to variational methods, promising results for estimating the state and basal conditions of ice sheets have been reported by Bonan et al. (2014) and Gillet-Chaulet (2020). These studies investigated the performance of EnKFs using idealized twin experiments where observations generated from a model run are used as synthetic observations to investigate this DA approach. This strategy has been further developed to



70



initialize a marine ice sheet model that includes the ice front and grounding line migration (Bonan et al., 2017; Gillet-Chaulet, 2020). However, these studies utilized simplified flowline models, limiting the representation of the horizontal stress field that can impact ice dynamic processes through, for example, buttressing.

Data assimilation and associated data denial experiments can be used to test the benefit of current observations, typically referred to as Observation System Experiments (OSEs), as well as to evaluate the potential benefits of proposed observations, typically referred to as Observation System Simulation Experiments (OSSEs) (OSSEs, Arnold Jr and Dey, 1986; Masutani et al., 2010). The main difference is that OSEs assimilate real observations, while OSSEs assimilate synthetic observations generated from model output with errors sampled from an appropriate observation error distribution. Both approaches aim to provide a systematic assessment of the value of observations for improving model state and parameter estimation. OSSEs have been successfully applied to atmospheric and oceanic models for decades, where analysis systems and the required DA frameworks are far more established (Boukabara et al., 2016; Hoffman and Atlas, 2016). For ice sheet modeling, however, the application of these OSE/OSSE approaches is still in the early stages of development.

This study explores the feasibility and benefits of using an EnKF to assimilate surface observations into a 2D plan-view ice model, with the aim of accurately estimating both the model state and key model parameters related to basal conditions (basal friction and topography). Using the shelfy-stream approximation (SSA, MacAyeal, 1989) for the stress balance of the ice sheet, ice thickness serves as the only prognostic variable representing the model state. Basal friction and topography, which cannot be directly measured, are treated as key model parameters that must instead be estimated through surface observations. We perform a twin experiment in which we evaluate the estimated state and parameters by comparing them with true reference values and using them as initial conditions to assess the impact of ensemble data assimilation on model projections. Our modeling settings are similar to those used in the previous study (Gillet-Chaulet, 2020) which used a flowline model, with necessary modifications for our model domain geometry and the coupling between a 2D ice sheet model and the data assimilation system. We investigate various ensemble DA parameters on a synthetic ice sheet domain to explore effective ensemble DA strategies relevant to ice sheet modeling. One of the primary objectives of this research is to use an idealized model configuration to help inform future efforts in applying an EnKF for real glacier cases. Within this context, we also configure Observing System Simulation Experiments (OSSEs) to evaluate the impact of various configurations of observations on the estimated model state and basal conditions. Section 2 describes the ice sheet model and data assimilation experimental setup along with the description of the different OSSEs that were performed. The results are presented in Section 3, followed by a discussion in Section 4.

85 2 Methods

In this study, we conduct a twin experiment to evaluate the performance of the ensemble DA framework for model initialization and projections. In addition, we perform Observing System Simulation Experiments (OSSEs) to explore the potential impact of assimilating different types of observations and associated uncertainties on the model initialization results.





Table 1. Parameters for the reference ice sheet domain

Parameter	Value	Description
$z_{b,deep}$	-720 m	Maximum depth of the bedrock topography
L_x	640 km	Domain length (along ice flow)
L_y	80 km	Domain width (across ice flow)
d_c	500 m	Depth of the trough compared with the side walls
w_c	24 km	Half-width of the trough
f_c	4 km	Characteristic width of the side walls of the channel

2.1 Model Setup

90 We use the Ice-sheet and Sea-level System Model (ISSM, Larour et al., 2012) to simulate the model state and forecast its evolution over time. ISSM is a parallelized finite element ice flow model with anisotropic mesh refinement capabilities, which allows efficient ensemble simulations of the ice sheets.

We construct our reference simulation using a bed geometry inspired by Asay-Davis et al. (2016) and Gillet-Chaulet (2020). The synthetic bed topography features large-scale overdeepening combined with added small-scale roughness. The general shape of the bed is defined as:

$$z_b(x,y) = \max \left[B_x(x) + B_y(y), z_{b,deep} \right] \tag{1}$$

$$B_x(x) = \begin{cases} 150 - 3x, & 0 \text{ km} \le x \le 350 \text{ km} \\ -900 + 5(x - 350), & 350 \text{ km} \le x \le 450 \text{ km} \\ -400 - 3(x - 450), & 450 \text{ km} \le x \le L_x \end{cases}$$
 (2)

$$B_y(y) = \frac{d_c}{1 + e^{-2(y - L_y/2 - w_c)/f_c}} + \frac{d_c}{1 + e^{2(y - L_y/2 + w_c)/f_c}}$$
(3)

where the parameter values used in these equations are given in Table 1. Following Gillet-Chaulet (2020), we add a roughness signal using a random midpoint displacement method (Fournier et al., 1982). We use this method at 100 m resolution with 10 recursions using an initial standard deviation of 500 m and a roughness factor of 0.7. The model domain spans 0 to 640 km in the x-direction and 0 to 80 km in the y-direction. This domain is discretized into approximately 27,000 elements using a triangular mesh with resolutions varying from 500 m near the coast to 10 km inland.

The basal friction coefficient follows a sinusoidal function similar to that used by Gillet-Chaulet (2020), comparable to the inferred friction coefficient in Thwaites Glacier of Antarctica in terms of both amplitude and spatial variations (Brondex et al., 2019; Gillet-Chaulet, 2020). In this study, we have adjusted this function for a 2D domain with an additional y-component:





$$C(x,y) = C_x(x) \times C_y(y) \tag{4}$$

$$C_x(x) = 0.02 + 0.005 \sin(\frac{1}{40} \frac{2\pi(x - L_x)}{L_x}) \sin(10 \frac{2\pi x}{L_x})$$
 (5)

$$C_y(y) = \sin(\pi \frac{(y - L_y)}{L_y}) + 2$$
 (6)

For the stress balance of an ice sheet, we use the shelfy-stream approximation (SSA, MacAyeal, 1989), which simplifies the Stokes equations for cases with a small aspect ratio and basal friction. The basal stress, τ_b , is described by the Weertman friction law for grounded ice:

$$\tau_b = C|u_b|^{\frac{1}{m}-1}u_b \tag{7}$$

where C is a friction coefficient, u_b the ice basal velocity, and m the velocity exponent set to 1/3 in this study.

The ice viscosity is defined using Glen's law (Glen, 1955):

$$\mu = \frac{B}{2\dot{\varepsilon}_e^{1-\frac{1}{n}}},\tag{8}$$

where B is the ice viscosity parameter, $\dot{\varepsilon}_e$ the effective strain rate, and n Glen's law exponent set equal to 3.

The position of the ice front is fixed at the end of the domain, and the evolution of the grounding line is simulated with a subelement grounding line parameterization (Seroussi et al., 2014).

We run the model until it reaches a steady state using a uniform surface accumulation rate of 0.3 m/yr, without any basal melting. After 25,000 years, the ice sheet stabilizes at a steady state, with a grounding line located approximately at x = 470 km along the center line of the glacier, just downstream of the region of overdeepening (Fig. 1). To introduce dynamic changes, we perturb this equilibrium state by instantaneously reducing the surface mass balance to -0.3 m/yr. We also introduce basal melting using a simple melt-depth parameterization, as described by Favier et al. (2014), setting the melt rate of 200 m/yr at a depth of 800 m. The model then runs for an additional 200 years, while keeping these surface and basal forcings constant. For the first 100 years, the grounding line retreats at a relatively slow pace, but the retreats accelerate after approximately 130 years (Fig. 2). We refer to this simulation as our reference simulation, from which we derive synthetic observations and reproduce the state and parameters through our ensemble DA framework. The setup of the reference simulation resembles an idealized Antarctic glacier. The DA simulations conducted in Section 2.3 and 2.4 represent part of this 200-year run and utilize the same forcings as this reference simulation.

2.2 Data assimilation

120

130

We use the Data Assimilation Research Testbed (DART, Anderson et al., 2009) to implement ensemble data assimilation with ISSM. DART provides various DA algorithms and modules to create a complete end-to-end DA framework. In this study, we utilize the Ensemble Adjustment Kalman Filter (EAKF, Anderson, 2001) algorithm within DART, which is a modified version of the Kalman filter (Kalman, 1960) and belongs to a class of deterministic ensemble square-root filters (Tippett et al., 2003).





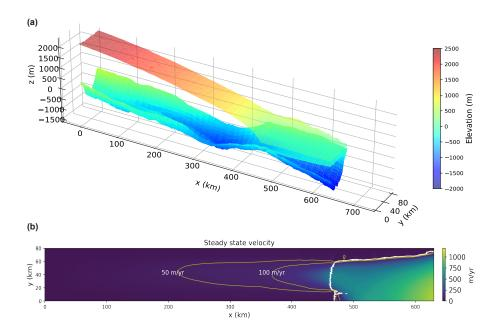


Figure 1. (a) Initial steady-state ice surface and basal elevation. (b) Initial steady-state velocity with contours of 50 m/yr and 100 m/yr (yellow lines). The white line shows the initial grounding line position.

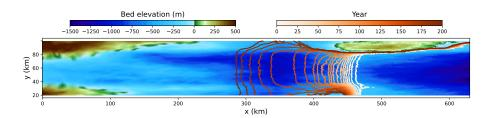


Figure 2. Bed topography of model domain and grounding line positions every 10 years from 0 to 200 years for the reference simulation (white to red).

The EAKF combines observations with an ensemble of model forecasts over a specified observation window to produce an ensemble of ice sheet analyses. In doing so, the EAKF incorporates a flow-dependent background and analysis error covariance that can be propagated to the next time of observations through an ensemble of model integration, which differs from a static background-error covariance typically used for variational data assimilation. DART places ice sheet variables into a state vector, then uses ensemble-estimated error covariance between the state vector and the state variables projected into observation space to compute the Kalman gain needed to update the model state. For the current study, the state vector in DART is augmented to include both the model state and the parameters that are updated through DA. Here, the augmented state vector includes ice thickness as a prognostic variable and friction coefficient and bed topography as model parameters to be estimated.



150

155

160

175



A common challenge with EnKFs is the issue of undersampling, which arises when the size of the ensemble is significantly smaller than the independently observed degrees of freedom for the model state. Localization and inflation are common methods to mitigate these issues and increase the stability of the filter (Carrassi et al., 2018; Morzfeld and Hodyss, 2023). Localization adjusts the spatial influence of observations, thereby preventing the distortion of estimates by distant observations. While previous studies (Gillet-Chaulet, 2020; Cook et al., 2023) have explored the effects of localization on state estimation using flowline models, its application to 2D plan-view models remains unexplored. Similarly, inflation, which addresses sampling errors by artificially increasing the forecast covariance matrix, has not been thoroughly studied for large-scale ice sheet modeling. To identify the most effective settings, we conduct sensitivity tests for both localization and inflation parameters to determine their optimal values for our ensemble data assimilation framework.

2.3 Twin experiment

We conduct a twin experiment to evaluate the performance of using an EnKF to assimilate surface observations into a 2D planview ice model. Using the ISSM-DART DA framework, we aim to estimate the ice sheet state together with model parameters. Here, we assume that the friction coefficient and the bed topography are the only two unknown parameters that need to be estimated, while all other parameters and forcings (e.g., ice rigidity, surface mass balance) are perfectly known and identical to those used in the reference simulation. We assimilate annual surface observations derived from the reference simulation over a 30-year span—approximately the satellite observational period for ice sheets—to assess the ability of the ensemble DA framework to recover the initial state and basal conditions of the reference ice sheet.

We obtain synthetic surface observations of ice elevation and velocities from the reference simulation and assume that the surface elevation and velocities are observed at annual resolution (e.g., at the start of each year) at each ISSM mesh node. To simulate observation error, we add uncorrelated Gaussian noise with a standard deviation of 5 m for the surface elevation and 10 m/yr for the velocity as a simple uncertainty baseline. These standard deviation values are lower than the ones from Gillet-Chaulet (2020), but still within a plausible range according to recent studies (Dai and Howat, 2017; Mouginot et al., 2017). We explore the sensitivity to the choice of applied uncertainties in our OSSEs below (Section 3.2).

To generate initial ensembles, we adopt an approach similar to that described by Gillet-Chaulet (2020). For the friction coefficient, we create a random field, assuming a known mean value of $2,500 \ Pa \ m^{-1/3} a^{1/3}$ across the domain and using a prescribed covariance model for spatial dependency. We use a Gaussian function for the variogram with a range of 5 km and a sill of 90,000. These values for the range and sill were selected based on Gillet-Chaulet (2020), with adjustments made for the domain and friction law used in this study. For bed topography, we use an exponential function for the variogram with a range of 50 km, a sill of $4,000 \ m^2$ and a nugget of $200 \ m^2$, also based on the same study (Gillet-Chaulet, 2020). Unlike the friction coefficient, which typically cannot be directly measured and often lacks prior knowledge, the bed topography can be measured using ice penetrating radar (e.g., Evans and Robin, 1966; Dowdeswell and Evans, 2004; Rodriguez-Morales et al., 2014). We assume that we have radar measurements of bed topography along tracks perpendicular to ice flow every 30 km. We generate a conditional random field of the bed topography, prescribed by these observations and the exponential covariance model. Initial ensembles for both parameters are created using the GSTools Python package (Müller et al., 2022). Additional initial ice sheet



180

210



variables, such as initial thickness and velocity, are calculated through a stress balance solution using the initial ensemble of friction coefficient and bed topography.

To date, no studies have determined optimal localization and inflation parameters for large-scale 2D ice sheet models. Therefore, we conduct sensitivity tests to identify the best values for these parameters across various ensemble sizes. For this study, a Gaspari-Cohn fifth-order polynomial is used for horizontal direction localization to limit observation updates within a specific radius (Gaspari and Cohn, 1999). For inflation, we use the spatially uniform state space inflation (Anderson et al., 2009). We explore various inflation and localization radii values to find the optimal combination. Initial experiments begin with an ensemble size of 30, based on findings from smaller-scale flowline model studies that demonstrate robust DA performance with relatively small ensembles. We then extend our experiments to larger ensembles, up to 100 members, to examine the impact of ensemble size on DA performance in large-scale ice sheet modeling.

To evaluate the effectiveness of the ensemble DA framework in retrieving basal conditions and ice sheet state, we calculate the root-mean-square error (RMSE) between the analysis mean states and the designated true values for bed topography (RMSE_B), friction coefficient (RMSE_C), and ice thickness (RMSE_H). After each analysis, RMSE values are computed at all nodes where basal conditions have been updated through assimilation. This calculation includes only those nodes where at least one node in the triangular mesh is grounded, as surface observations only respond to changes in the basal condition of grounded ice.

2.4 Observing System Simulation Experiments (OSSEs)

We conduct Observing System Simulation Experiments (OSSEs) within our synthetic model domain to investigate the potential impact of varying observed quantities and their associated uncertainties. For our OSSEs, we assume a "perfect" model without any model error, following the perfect model OSSE framework (Zhang et al., 2018). While the twin experiment described in the previous section is more focused on testing the capabilities of ensemble Kalman filter data assimilation system under ideal conditions, the suite of experiments in this section is designed to explore the feasibility of performing joint state-parameter estimation for the ice sheet model under realistic observational settings, which will provide valuable insight and guidance for future, more realistic OSSE efforts. In this study, we primarily explore the impact of different types of surface elevation observations and their uncertainties. We assimilate the synthetic elevation data in two different ways: i) along ground tracks, which mimics The Ice, Cloud, and Land Elevation Satellite-2 (ICESat-2) ATL11 product, ii) at regularly gridded locations, which mimics the ICESat-2 ATL15 product (Smith et al., 2023, 2024). We use the same velocity data as in the previous twin experiment, assuming that the velocity products provide almost full coverage of annual velocity both spatially and temporally, and we focus on the impact of surface elevation observations.

For the along-track data, we generate synthetic surface elevation observations along tracks that emulate the Reference Ground Track (RGT) used by ICESat-2 ATL11 product. The RGT is a virtual line that corresponds to the nadir track of the designed orbit (Smith et al., 2019). For our synthetic domain, surface elevation is assumed to be observed annually, while the actual temporal resolution of ATL11 data is 91 days. Synthetic observations are spaced every 60 m along each track, which is the spatial resolution of ATL11 ice height data (Smith et al., 2023). While the actual ATL11 product exhibits varying cross-





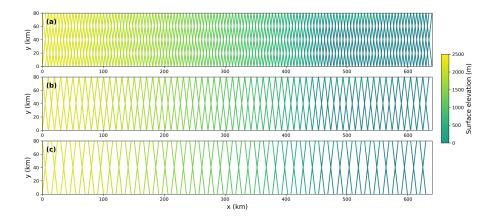


Figure 3. Elevation observations taken along synthetic ground tracks from a configuration of (a) 5 km cross-track spacing, (b) 10 km cross-track spacing, and (c) 15 km cross-track spacing, with data points posted every 60 m along the track.

track spacing depending on latitude, we test cross-track spacings from 5 to 15 km, which covers the range of cross-track spacing of the ICESat-2 RGTs in the polar regions (Fig. 3). To generate synthetic observations, we linearly interpolate model surface elevation at surrounding mesh nodes to the observation points along our tracks. We also explore the impact of the observational uncertainties on the DA performance by conducting experiments with different levels of uncertainty in surface elevation. These experiments aim to determine the permissible level of error for different surface elevation products to ensure reliable DA for our model domain. We introduce Gaussian noise to surface elevation at each mesh node, using standard deviation ranging from 5 to 20 m with 5 m increments, and propagate standard errors to points along the tracks.

For gridded elevation observations, we create synthetic datasets at 1 km, 10 km and 20 km resolutions, corresponding to the spatial resolution of ATL15 product. The ATL15 product is a spatially continuous gridded dataset of land ice height-change (Smith et al., 2024). We first interpolate surface elevation from the reference model mesh onto a grid with 100 m resolution, then average these 100 m grids to create 1 km grid cell, using equal weights for all 100 m grids. Surface elevation data at 10 km and 20 km resolutions are created similarly from 1 km grid data. In our OSSEs, we assume an annual observation frequency of surface elevation for the consistency across experiments, including the twin experiments, although the actual temporal resolution of ATL15 data is 91 days. Similar to the track elevation data, Gaussian noise is introduced with standard deviations from 5 to 20 m at each mesh node, with propagated error onto the gridded data.

3 Results

215

220

225

3.1 Twin experiments and projections

Our twin experiments show the feasibility of the EnKF DA approach for ice flow modeling. The experiments were conducted with a range of configurations. We explored ensemble sizes of 30, 50 and 100, varying the localization radius from 2 to 20 km



240

245

255

260

265



in 2 km increments and adjusting the inflation parameters from 1 to 1.2 in 0.02 intervals. Fig. 4 shows the RMSE values for the bed topography, friction coefficient, and ice thickness after 30 years of DA. As the ensemble size increases, DA performance remains relatively robust—demonstrated by lower RMSEs—over a wider range of localization radii and inflation parameters. We observed that the best DA results, indicated by the minimum RMSEs, were achieved with a localization radius of 4 km for the friction coefficient and 6 km for bed topography and ice thickness. When the localization radius was set below those optimal values (4 km for friction coefficient and 6 km for bed topography and ice thickness), a significant increase in RMSEs occurred, and any increase beyond those optimal values also resulted in gradual increases in RMSEs. As expected, the optimal inflation parameters tend to decrease as the ensemble size increases, resulting in values between 1.10 - 1.14 for the friction coefficient and 1.16 - 1.18 for bed topography and ice thickness when using the optimal radius for each parameter. Additionally, with the optimal localization radius, we noted an improvement in DA performance with increasing inflation parameters up to a certain threshold, beyond which the performance significantly decreased.

To assess the impact of ensemble size, we compare the evolution of RMSEs as a function of assimilation time using the optimal localization and inflation parameters identified above (Fig. 4). For the friction coefficient, RMSE decreases rapidly during the first 5 years and continues to decrease steadily until the end of the assimilation window. The RMSE values of bed topography and ice thickness show a relatively steady decrease across all tested ensemble sizes. The simulations with larger ensemble sizes show an improvement in DA performance compared to an ensemble size of 30, but the benefits saturate as the ensemble size increases from 50 to 100. For the remaining experiments in this study, we proceed with an ensemble size of 50, a localization radius of 4 km and an inflation parameter of 1.12.

The reference friction coefficient and bed topography, along with the ensemble mean fields, before and after assimilation from our optimal DA configuration, are shown in Fig. 6 and Fig. 7. We also show the changes in difference between true ice thickness and the ensemble mean ice before and after assimilation in Fig. 8. As more observations are assimilated, the discrepancies from the reference fields decrease compared to the initial ensemble mean. The areas around the grounding line, where the signal-to-noise ratio of velocity is relatively high, exhibit the most significant improvements through ensemble DA. In these regions, the spatial variations of both the friction coefficient and bed topography fields are accurately captured by the ensemble DA process. At the end of the 30-year assimilation period, areas located far upstream (up to 350 km) from the grounding line continue to show improvements, while not as significant as those observed near the grounding line.

Based on the state and parameters estimated from the DA simulation, we conducted deterministic and ensemble forecasts extending up to t = 200 yr to explore the impact of ensemble DA initialization on model projections. We used the ensemble mean for the deterministic simulation and the full ensemble for the ensemble forecast simulations, similar to Gillet-Chaulet (2020). We also utilized the estimated state and parameters as initial conditions from various points in the DA simulation different initial conditions, e.g., the analyzed states at t = 5 yr, t = 15 yr, and t = 30 yr, for forecast simulations to investigate the impact of different DA periods on model simulations. Figure 9 presents the changes in ice volume over time for the reference simulation, along with the forecast simulations based on the ice sheet state with and without data assimilation over periods of 5 to 30 years. Without data assimilation, the deterministic forecast—using the ensemble mean basal conditions—tends to underestimate ice loss over the 200-year period. This simulation, however, captures the accelerated volume loss observed in





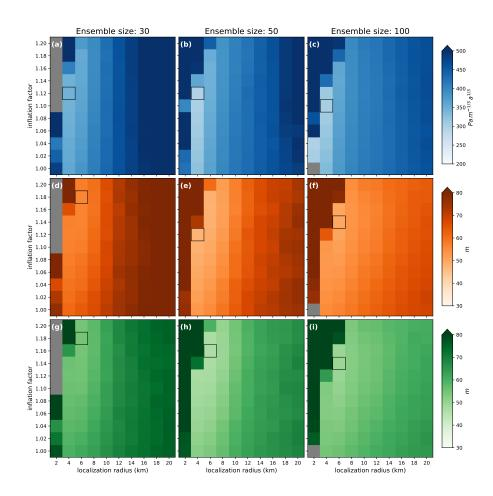


Figure 4. The root-mean-square error (RMSE) between the analysis mean and the reference at t = 30 years as a function of the inflation factor and the localization radius for different ensemble sizes. (a-c) friction coefficient, (d-f) bed elevation, and (g-i) ice thickness. The grey indicates experiments that diverge by t = 30 years. The black box in each panel represents the location of minimum RMSE.

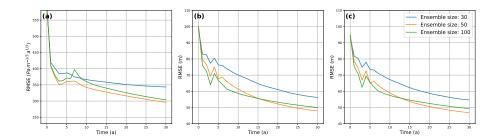


Figure 5. The evolution of mean analysis RMSE for (a) friction coefficient and (b) bed topography using three different ensemble sizes. Each plot uses the localization radius and inflation factor that produce the minimum RMSE at t = 30 yr (Fig. 4).





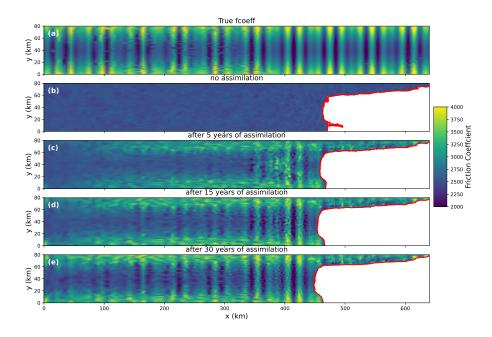


Figure 6. (a) Reference friction coefficient (i.e., truth), (b) the ensemble mean friction coefficient before assimilation, (c)-(e) the ensemble mean friction coefficient after (c) 5 years, (d) 15 years and (e) 30 years of assimilation. The localization radius is set to 4 km and the inflation factor is 1.12 with the ensemble size of 50. The red lines show the grounding line positions.

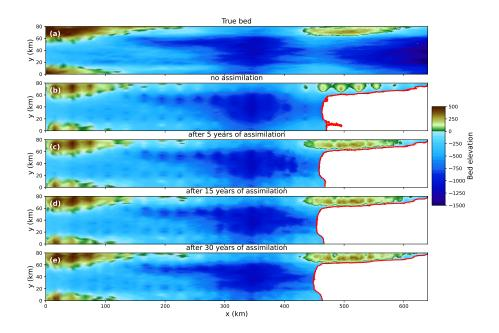


Figure 7. Same as Fig. 6 but for bed topography.



275



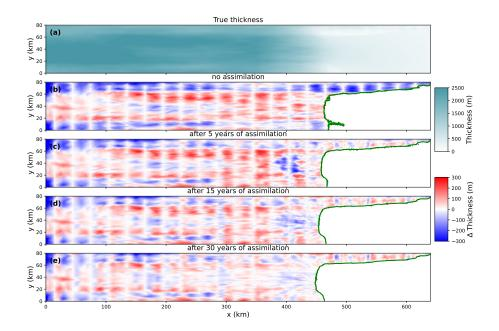


Figure 8. (a) Reference ice thickness (i.e., true) at t = 0 yr, (b) difference between true ice thickness and the ensemble mean ice thickness before assimilation (true - ensemble mean), (c)-(e) difference between true ice thickness and the corresponding ensemble mean ice thickness at (c) 5 years, (d) 15 years and (e) 30 years after assimilation. The localization radius is set to 4 km and the inflation factor is 1.12 with the ensemble size of 50. The green lines show the grounding line positions.

the reference simulation beginning at t = 130 yr, when the grounding line enters the reverse-sloping bed topography. By the end of the forecast simulation, the discrepancy in volume loss between the reference and deterministic simulations is 2,700 Gt. Across the ensemble members, the changes in ice volume at t = 200 yr range from 7,300 Gt to 29,600 Gt, with only about 25 % of entire members successfully predicting the onset of accelerated volume loss at t = 130 years.

As more observations are assimilated, the ensemble spread is reduced, and the results of the deterministic simulations more closely align with the reference simulation. After 5 years of assimilation, both the deterministic and ensemble forecast simulations accurately reproduce changes in ice volume up to t = 15 years before beginning to diverge from the reference trajectory, resulting in 3,800 Gt of difference in volume loss by the end of the forecast period. After the 15 years of assimilation, the deterministic forecasts closely match the reference volume loss up to approximately t = 100 years, although these forecasts lose more mass from t = 100 to t = 200 years compared to the reference simulation. Extending the data assimilation period up to 30 years further decreases errors in the ensemble mean over the 200-year period, while consistently decreasing the ensemble spread.





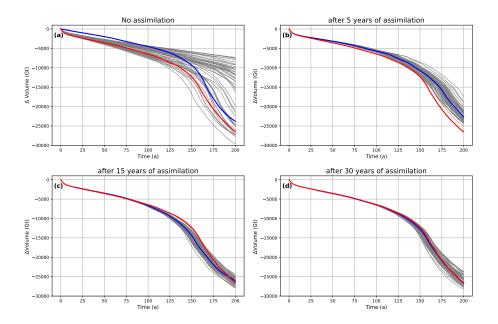


Figure 9. Changes in ice volume from ensemble forecast simulations with (a) no assimilation, (b) assimilation up to 5 years, (c) assimilation up to 15 years, and (d) assimilation up to 30 years. The red line shows the reference run and the blue line shows the forecast simulation with the mean ensemble state. The gray lines show the forecast simulation of each ensemble member.

3.2 OSSEs

280

285

290

In the context of our Observing System Simulation Experiments (OSSEs), we evaluate the impact of varying cross-track spacings and grid resolutions of surface elevation data on the performance of DA in estimating the model state and parameters. Since the simulated surface elevation observations use different cross-track spacings and grid resolutions, we conduct sensitivity tests with an ensemble size of 50 to optimize both localization and inflation parameters. When assimilating along-track surface elevations with 5 km and 10 km across track spacing, the best DA results were achieved with a localization radius of 4 km and the inflation parameters between 1.10 and 1.14 for all variables (Fig. 10), similar to the DA results with full coverage of elevation data at each model mesh node in the twin experiment. As the across-track spacing increases to 10 - 15 km, the overall DA performance declines due to suboptimal choices for inflation and localization parameters, indicated by an increase in the mean RMSE by up to 16 % for three estimated variables. For the gridded elevation data with 1 km resolution, the optimal localization and inflation parameters are 4 km and 1.12, respectively, for all variables. In experiments with gridded elevation data of 10 km and 20 km resolutions, the overall DA performance declines (i.e., an increase in RMSE) over a range localization and inflation parameters. We find the minimum RMSE values at the end of the assimilation window with a localization radius of 6 - 8 km and inflation values of 1.02 - 1.06 for both 10 km and 20 km resolution data (Fig. 11).

With the optimal parameter combinations identified for each elevation data type experiment, we conducted additional experiments exploring the impact of the prescribed uncertainty (σ_h) of surface elevation data. To evaluate the DA performance, we



300



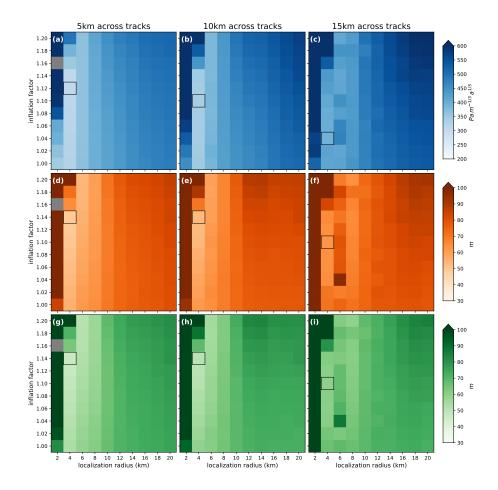


Figure 10. Analysis ensemble mean RMSEs at t = 30 years as a function of the inflation factor and the localization radius for different across-track spacing of elevation data for (a-c) friction coefficient, (d-f) bed elevation, and (g-i) ice thickness. The grey shading indicates experiments that diverge by t = 30 yrs. The black box in each panel represents the minimum RMSE for each configuration.

summarized the RMSEs at the end of the assimilation window (at year 30) for each experiment in Table 2 and 3. The evolution of RMSEs over the assimilation period using the ground track and grid elevation observations are shown in Fig. 12 and 13, respectively.

When assimilating observations with 5 km across-track spacing and the same observational error as in the twin experiments ($\sigma_h = 5 m$ and $\sigma_v = 10 m/yr$), the DA performance, as measured by RMSEs, is comparable to that observed in the twin experiment. As the across-track spacing of observed surface elevation increases, DA performance declines as expected. When assimilating data at 10 km or 15 km across-track spacing, RMSE values remain higher than those with 5 km spacing at t = 30 years, although RMSE values continue to decrease until the end of the assimilation window. A similar result is observed with gridded elevation observations: high-resolution data (1 km) produces DA performance comparable to that of the twin experiment. However, as the spatial resolution increases to 10 km and 20 km, the overall DA performance declines, with only



310



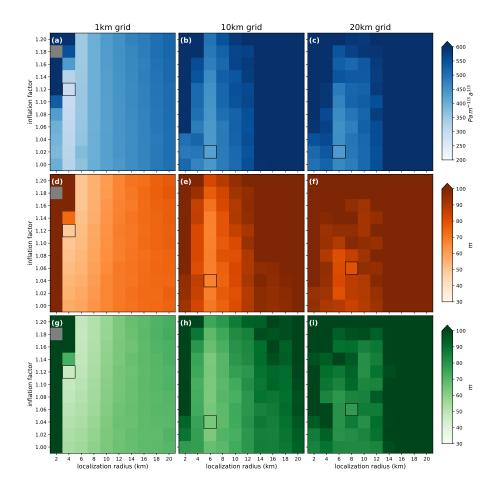


Figure 11. Same as Fig. 10 but for different grid resolution of elevation data.

marginal improvements in parameter and state estimations after 10 - 15 years of assimilation. These results indicates that the resolution of the elevation data can have a significant impact on ice sheet DA performance.

With 5 km across-track spacing, DA performance decreases as the uncertainty in the surface observation increases. This decrease in performance is more pronounced in retrieving bed topography and ice thickness compared to the friction coefficient. With the 10 km across-track data, DA performance remains consistent for all three estimated variables across all uncertainty levels in elevation data, as RMSE values continue to decrease throughout the assimilation window. When using the 15 km across-track data, only surface elevation with an observational error of 5 m improves bed and ice thickness estimation up to t = 30 years, while prescribed errors of 10 - 20 m did not yield further improvements beyond 15 - 20 years of DA. With the 1 km gridded elevation data, increasing uncertainty levels reduce the accuracy of bed and ice thickness estimation. With coarser grid data (10 km and 20 km), however, the DA performance does not vary significantly across different uncertainty levels.





Table 2. List of experiments using various across-track surface observations and analysis mean RMSEs t = 30 years.

Experiment Name	RMSE_C ($Pa m^{-1/3} a^{1/3}$)	RMSE_B (m)	RMSE_H (m)
Twin experiment ($\sigma_h = 5 \text{ m}$ and $\sigma_v = 10 \text{ m/yr}$)	296.01	47.63	46.87
Track_5km_ σ_h _5_ σ_v _10	306.89	49.06	47.77
Track_5km_ σ_h _10_ σ_v _10	304.96	50.65	48.96
Track_5km_ σ_h _15_ σ_v _10	305.62	51.71	50.14
Track_5km_ σ_h _20_ σ_v _10	313.61	54.02	52.56
Track_ 10 km_ σ_h _ 5 _ σ_v _ 10	338.28	53.69	51.18
Track_ 10 km_ σ_h _ 10 _ σ_v _ 10	335.26	52.84	50.62
${\rm Track_10km_}\sigma_h_{\rm 15_}\sigma_v_{\rm 10}$	350.69	56.86	53.19
Track_10km_ σ_h _20_ σ_v _10	341.78	56.45	54.17
Track_15km_ σ_h _5_ σ_v _10	410.10	62.79	59.59
Track_15km_ σ_h _10_ σ_v _10	429.70	73.43	70.03
Track_15km_ σ_h _15_ σ_v _10	414.05	72.55	65.96
Track_15km_ σ_h _20_ σ_v _10	389.90	69.62	65.74

4 Discussion

In this study, we have shown that the EnKF can effectively improve the accuracy of model state estimates for a semi-idealized glacier, especially in fast-flowing regions. These results are consistent with those from previous studies (Gillet-Chaulet, 2020; Bonan et al., 2014, 2017), yet our approach employs a 2D model with unstructured meshes, enhancing its applicability to larger-scale ice sheet modeling simulations. Similar to earlier studies, assimilating new observations over the first few years significantly improves the accuracy of bed topography, friction coefficient and ice thickness estimates in fast-flowing regions.

Although the slow-flowing regions—where the relative error in velocity observation is higher than in fast-flowing regions—show only limited improvements in basal conditions compared to the fast-flowing region, they still show notable improvements up to 300 km inland from the initial grounding lines (x = 150 km). These improvements allow accurate forecasts of ice volume loss for up to 200 years, as the grounding line retreats by approximately 150 km (to x = 300 km) by the end of the reference simulation.

The initial ensembles for the model parameters—bed topography and friction coefficient—cannot be generated by the commonly used methods for atmospheric or ocean modeling, which typically rely on perturbations of initial conditions with boundary conditions from meteorological forcing. Instead, we assume reasonably accurate prior knowledge of initial conditions and prescribe covariance models to establish spatial correlation for both parameters. In real glacier applications, however, these assumptions may not hold. For better DA results, more accurate measurements and/or prior information for bed conditions





Table 3. List of experiments using various gridded surface observations and analysis mean RMSEs at t = 30 years.

Experiment Name	RMSE_C ($Pa m^{-1/3} a^{1/3}$)	RMSE_B (m)	RMSE_H (m)
Twin experiment ($\sigma_h = 5 \text{ m}$ and $\sigma_v = 10 \text{ m/yr}$)	296.01	47.63	46.87
Grid_1km_ σ_h _5_ σ_v _10	291.38	48.65	46.81
Grid_1km_ σ_h _10_ σ_v _10	288.54	48.62	47.43
Grid_1km_ σ_h _15_ σ_v _10	291.29	53.89	53.14
Grid_1km_ σ_h _20_ σ_v _10	290.66	54.88	53.97
Grid_10km_ σ_h _5_ σ_v _10	437.48	67.58	63.72
Grid_10km_ σ_h _10_ σ_v _10	423.84	66.76	63.99
Grid_10km_ σ_h _15_ σ_v _10	430.58	65.96	62.63
$Grid_10km_\sigma_h_20_\sigma_v_10$	427.20	66.61	63.20
Grid_20km_ σ_h _5_ σ_v _10	410.10	80.07	80.76
$\mathrm{Grid}_20\mathrm{km}_\sigma_h_10_\sigma_v_10$	429.70	80.69	79.96
Grid_20km_ σ_h _15_ σ_v _10	414.05	77.42	78.97
Grid_20km_ σ_h _20_ σ_v _10	389.90	77.84	79.39

are required, such as additional radar measurements of bed topography and potential relationships between geophysical observations (e.g., seismic or radar-based measures) and friction (Kyrke-Smith et al., 2017; Haris et al., 2024). Alternatively, multi-model reconstructions of parameters could be leveraged to generate initial ensembles and determine the spread (Gillet-Chaulet, 2020). Our DA results, along with localization and inflation factors, depend on assumptions on the initial ensemble. Exploring how gaps in prior information affect DA results could also provide valuable insights, particularly in understanding the robustness of DA results when challenged with realistic data limitations and parameter uncertainties.

The robust performance of EnKF in constraining the basal conditions and initial ice sheet state for future projection has been achieved with a relatively small ensemble size, consistent with previous studies performing data assimilation for flowline models. We further show that increasing the ensemble size allows robust DA performance over a wider range of localization radii and inflation parameters and produces only marginally improved performance in retrieving basal conditions with shorter assimilation windows. Therefore, a majority of experiments performed in this study use an ensemble size of only 50 members, which we find to be a reasonable tradeoff between data assimilation accuracy and computational efficiency. Nonetheless, for cases with unknown DA parameters, particularly in smaller domains, a larger ensemble size could prove advantageous. Further studies are needed to identify the optimal approach for implementing an EnKF for real observations.

Inflation and localization techniques have been used to stabilize the filter, similar to previous studies (Bonan et al., 2014; Gillet-Chaulet, 2020). The optimal inflation factors for this study (1.10 - 1.18) are similar to values from earlier studies. For localization radius, the best results were obtained with a radius of 4 - 8 km, compared to previous flowline model studies



355

360



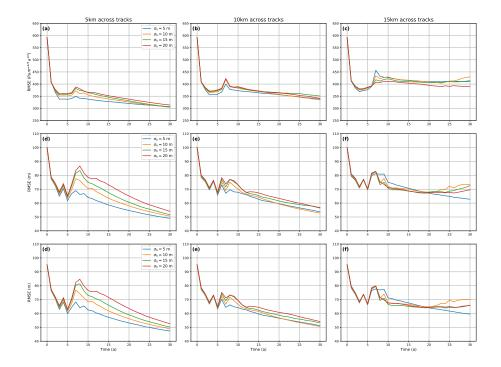


Figure 12. The evolution of ensemble mean RMSEs using different across-track spacing surface elevation with various uncertainties on observations for (a-c) friction coefficient and (d-f) bed topography.

that suggested a wider range (4 - 120 km) depending on the grid size (Bonan et al., 2014; Gillet-Chaulet, 2020). Given our use of a 2D unstructured mesh, adaptive inflation (El Gharamti, 2018) and localization (Bishop and Hodyss, 2007) can be viable alternatives, as each node has a different number of observations to be assimilated. Future research should explore these methods with real observations varying in resolution and spatial density.

In our twin experiment and projections, we find that assimilating more observations to estimate basal conditions improves the accuracy of model projections from the estimated states. Assimilating surface observations for up to 15 years results in ensemble and deterministic ice volume loss forecasts that closely match the reference simulation for up to 100 years, with much reduced ensemble spread and ice volume loss difference limited to approximately XX Gt (compared to XX Gt with no assimilation). Extending the assimilation window to 30 years allows forecast simulations to match the reference simulation for up to 200 years. Our projections further show a better match to the reference simulations compared to those from a previous study (Gillet-Chaulet, 2020), potentially due to our use of more observations with smaller error variance (σ_v and σ_h). The method used in this study that assimilates time series of observations maintains consistency with transient changes, providing an optimal initial condition for changing glaciers. Further studies involving real glaciers could extend this method to ice-sheet-wide-scale models, improving their capability to accurately estimate the current state and future changes in ice sheets.

The purpose of our OSSE experiments in this study is to demonstrate the capabilities of OSSEs within the ISSM-EnKF framework. Our OSSE experiments show that an EnKF can effectively assimilate various types of surface elevation obser-



370

375



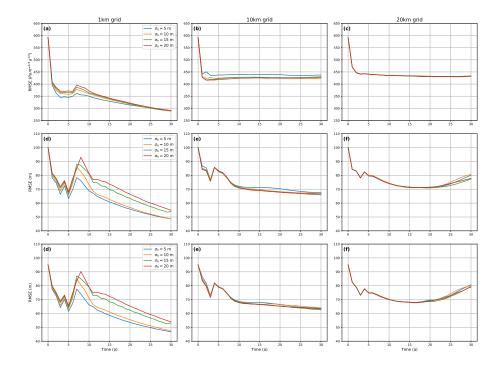


Figure 13. Same as Fig 13 but with different grid resolution for surface elevation observations.

vations (both grid and track) to evaluate the impact of different observational products. The results highlight that the spatial resolution of surface elevation data is crucial in determining the effectiveness of DA for estimating ice sheet model parameters and state (Table 2 and 3). The observed decline in DA performance with increased across-track spacing (from 5 km to 15 km) and grid size (from 1 km to 20 km) alludes to the benefits of high-resolution elevation data for initializing ice sheets. While the EnKF still performs reasonably well with larger spacings and coarser grids, the reduced spatial resolution limits its ability to fully capture the glacier state, emphasizing the need for a balance between observational density and coverage to maximize DA performance over the historical period. Additionally, the marginal improvements observed at coarser resolutions (10 km and 20 km) after 10–15 years suggest that, beyond a certain spatial threshold, additional data points do not substantially improve long-term parameter and state estimations (Fig. 12 and 13).

The OSSE experiments also provide a basic demonstration of the impact of observational error on DA performance, with particular benefits of lower uncertainties on bed topography and ice thickness estimation, while friction coefficient retrieval appears less sensitive to the prescribed surface elevation uncertainty. With our semi-idealized model domain and simplified error propagation method for surface elevation, we do not derive specific error thresholds for effective ice sheet model parameters and state estimation. However, we note that a proper specification of observation uncertainty is likely critical for the EnKF to produce accurate state and parameter estimates. Future OSSE experiments will target real glaciers with different observational specifications, which can contribute to the planning of future observational missions.



380

385

390

400

405



Despite the promising results demonstrated in this study, several limitations exist that must be acknowledged and addressed in future research. First, our study utilized yearly synthetic observations with uniformly homogeneous error variance, which do not fully capture the complexities and variability present in real observations. In addition, we assumed full spatial and temporal coverage of velocity data to isolate and focus on the impact of surface elevation observations. While this simplifies the analysis, it is an idealized scenario; future research should explore more realistic data scenarios, including partial velocity coverage, and assess the trade-offs between observation density, cost, and assimilation performance. A joint cost and benefit analysis of surface and velocity observations would provide a more robust understanding of their relative contributions to improving model estimates. Future research should also consider more sophisticated methods to account for observations from diverse sensors, coverage, varying periods, state dependence, and collection frequencies, as well as their associated error covariance matrices. This includes conducting more comprehensive OSSEs with a broader range of potential observations.

Additionally, this study focused on only one filter algorithm with a limited range of inflation and localization parameters, which may not adequately explore the full potential and scalability of the DA method. Future studies should investigate different types of filter algorithms and a variety of inflation and localization techniques to better optimize the assimilation process for ice sheet modeling. Furthermore, incorporating more comprehensive climate processes could enhance the predictive capabilities of our simulations. For example, integrating the firn process into the model could help not only in accurately modeling the grounding line position (Gillet-Chaulet, 2020) but also in properly determining observation errors in the DA process.

395 5 Conclusions

In this study, we introduce an ensemble Kalman filter-based data assimilation (DA) framework to calibrate a 2D plan-view ice model. Using a synthetic twin experiment, we showed that the ensemble DA method effectively recovers basal conditions (friction coefficient and bed topography) and ice thickness after several assimilation cycles. Assimilating more observations improves the accuracy of the model state as expected. The model state with assimilation of surface observations up to 30 years reproduced projected changes in ice volume of the reference simulation for up to 200 years with great accuracy. We also conduct Observing System Simulation Experiments (OSSEs) using the same model domain as the twin experiment but with synthetic elevation observations along ground track and gridded data that emulate the ICESat-2 ATL11 and ATL15 products, respectively. These experiments presented the potential surface elevation product that can be used to accurately estimate bed conditions and the model state of the idealized glacier. Different levels of observational uncertainty could improve the assimilation results, which highlights the importance of a more accurate representation of observation uncertainty in the DA process. The ensemble DA framework, which assimilates observations from multiple time points, holds significant potential for application to real glaciers to better estimate the current and future changes in ice sheet state variables. This framework also provides advantages for OSSEs aimed at testing various observational settings, as it requires less numerical effort than variational methods that assimilate time series of observations, making it a practical and effective tool in ice sheet modeling.





410 Code and data availability. The ISSM is open source and the source code of ISSM is available at https://github.com/ISSMteam/ISSM. The source code of DART is available at https://github.com/NCAR/DART (DART, 2024). The script for the results and figures are available at https://doi.org/10.5281/zenodo.14722078.

Author contributions. YC designed the experiments and conducted all simulations with help from AP, DF and JP. YC drafted the initial manuscript with inputs from AP, and all authors contributed to editing the manuscript.

115 Competing interests. The contact author has declared that none of the authors has any competing interests.

Acknowledgements. This work was supported by NASA under a Decadal Survey Incubation (DSI) Surface Topography and Vegetation team award (#80NSSC22K1112).





References

435

- Anderson, J., Hoar, T., Raeder, K., Liu, H., Collins, N., Torn, R., and Avellano, A.: The data assimilation research testbed: A community facility, Bull. Am. Meteorol. Soc., 90, 1283–1296, 2009.
 - Anderson, J. L.: An ensemble adjustment Kalman filter for data assimilation, Mon. Weather Rev., 129, 2884–2903, 2001.
 - Arnold Jr, C. P. and Dey, C. H.: Observing-systems simulation experiments: Past, present, and future, Bull. Am. Meteorol. Soc., 67, 687–695, 1986.
- Asay-Davis, X. S., Cornford, S. L., Durand, G., Galton-Fenzi, B. K., Gladstone, R. M., Gudmundsson, G. H., Hattermann, T., Holland, D. M., Holland, D., Holland, P. R., et al.: Experimental design for three interrelated marine ice sheet and ocean model intercomparison projects: MISMIP v. 3 (MISMIP+), ISOMIP v. 2 (ISOMIP+) and MISOMIP v. 1 (MISOMIP1), Geosci. Model Dev., 9, 2471–2497, 2016.
 - Bishop, C. H. and Hodyss, D.: Flow-adaptive moderation of spurious ensemble correlations and its use in ensemble-based data assimilation, Q. J. R. Meteorol. Socy., 133, 2029–2044, 2007.
- Bonan, B., Nodet, M., Ritz, C., and Peyaud, V.: An ETKF approach for initial state and parameter estimation in ice sheet modelling, Nonlinear Process. Geophys., 21, 569–582, 2014.
 - Bonan, B., Nichols, N. K., Baines, M. J., and Partridge, D.: Data assimilation for moving mesh methods with an application to ice sheet modelling, Nonlinear Process. Geophys., 24, 515–534, 2017.
 - Boukabara, S.-A., Moradi, I., Atlas, R., Casey, S. P., Cucurull, L., Hoffman, R. N., Ide, K., Kumar, V. K., Li, R., Li, Z., et al.: Community global observing system simulation experiment (OSSE) package (CGOP): description and usage, J. Atmos. Ocean. Technol., 33, 1759–1777, 2016.
 - Brondex, J., Gillet-Chaulet, F., and Gagliardini, O.: Sensitivity of centennial mass loss projections of the Amundsen basin to the friction law, Cryosphere, 13, 177–195, 2019.
 - Carrassi, A., Bocquet, M., Bertino, L., and Evensen, G.: Data assimilation in the geosciences: An overview of methods, issues, and perspectives, Wiley Interdiscip. Rev. Clim. Change, 9, e535, 2018.
- Choi, Y., Seroussi, H., Morlighem, M., Schlegel, N.-J., and Gardner, A.: Impact of time-dependent data assimilation on ice flow model initialization and projections: a case study of Kjer Glacier, Greenland, Cryosphere, 17, 5499–5517, 2023.
 - Cook, S., Gillet-Chaulet, F., and Fürst, J.: Robust reconstruction of glacier beds using transient 2D assimilation with Stokes, J. Glaciol., 69, 1393–1402, 2023.
- Dai, C. and Howat, I. M.: Measuring lava flows with ArcticDEM: Application to the 2012–2013 eruption of Tolbachik, Kamchatka, Geophys.

 Res. Lett., 44, 12–133, 2017.
 - DART: The Data Assimilation Research Testbed (Version 11.8.0) [Software], https://doi.org/10.5065/D6WQ0202, 2024.
 - Dowdeswell, J. A. and Evans, S.: Investigations of the form and flow of ice sheets and glaciers using radio-echo sounding, Rep. Prog. Phys., 67, 1821, 2004.
 - El Gharamti, M.: Enhanced adaptive inflation algorithm for ensemble filters, Mon. Wea. Rev., 146, 623-640, 2018.
- 450 Evans, S. and Robin, G. d. Q.: Glacier depth-sounding from air, Nature, 210, 883–885, 1966.
 - Favier, L., Durand, G., Cornford, S. L., Gudmundsson, G. H., Gagliardini, O., Gillet-Chaulet, F., Zwinger, T., Payne, A. J., and Le Brocq, A. M.: Retreat of Pine Island Glacier controlled by marine ice-sheet instability, Nat. Clim. Change, 4, 117–121, 2014.
 - Fournier, A., Fussell, D., and Carpenter, L.: Computer rendering of stochastic models, Commun. ACM, 25, 371-384, 1982.
 - Gaspari, G. and Cohn, S. E.: Construction of correlation functions in two and three dimensions, Q. J. R. Meteorol. Soc., 125, 723-757, 1999.





- 455 Gillet-Chaulet, F.: Assimilation of surface observations in a transient marine ice sheet model using an ensemble Kalman filter, Cryosphere, 14, 811–832, 2020.
 - Gillet-Chaulet, F., Gagliardini, O., Seddik, H., Nodet, M., Durand, G., Ritz, C., Zwinger, T., Greve, R., and Vaughan, D. G.: Greenland Ice Sheet contribution to sea-level rise from a new-generation ice-sheet model, Cryosphere, 6, 1561–1576, 2012.
 - Glen, J. W.: The creep of polycrystalline ice, Proc. R. Soc. A, 228, 519–538, 1955.
- Goelzer, H., Nowicki, S., Payne, A., Larour, E., Seroussi, H., Lipscomb, W. H., Gregory, J., Abe-Ouchi, A., Shepherd, A., Simon, E., Agosta, C., Alexander, P., Aschwanden, A., Barthel, A., Calov, R., Chambers, C., Choi, Y., Cuzzone, J., C., D., Edwards, T., Felikson, D., Fettweis, X., Golledge, N. R., Greve, R., Humbert, A., Huybrechts, P., Le clec'h, S., Lee, V., Leguy, G., Little, C., Lowry, D. P., Morlighem, M., Nias, I., Quiquet, A., Rückamp, M., Schlegel, N.-J.and Slater, D. A., Smith, R. S., Straneo, F., Tarasov, L., van de Wal, R., and van den Broeke, M.: The future sea-level contribution of the Greenland ice sheet: a multi-model ensemble study of ISMIP6, Cryosphere, 2020.
- Goldberg, D. N. and Heimbach, P.: Parameter and state estimation with a time-dependent adjoint marine ice sheet model, Cryosphere, 17, 1659–1678, 2013.
 - Goldberg, D. N., Heimbach, P., Joughin, I., and Smith, B.: Committed retreat of Smith, Pope, and Kohler Glaciers over the next 30 years inferred by transient model calibration, Cryosphere, 9, 2429–2446, 2015.
- Haris, R., Chu, W., and Robel, A.: What can radar-based measures of subglacial hydrology tell us about basal shear stress? A case study at Thwaites Glacier, West Antarctica, J. Glaciol., pp. 1–9, 2024.
 - Hoffman, R. N. and Atlas, R.: Future observing system simulation experiments, Bull. Am. Meteorol. Soc., 97, 1601-1616, 2016.
 - Iglesias, M. A., Law, K. J., and Stuart, A. M.: Ensemble Kalman methods for inverse problems, Inverse Probl., 29, 045 001, 2013.
 - Intergovernmental Panel on Climate Change (IPCC): Ocean, Cryosphere and Sea Level Change, pp. 1211–1362, Cambridge University Press, 2023.
- 475 Kalman, R. E.: A new approach to linear filtering and prediction problems, J. Fluids Eng., 82, 35–45, 1960.
 - Kyrke-Smith, T. M., Gudmundsson, G. H., and Farrell, P. E.: Can seismic observations of bed conditions on ice streams help constrain parameters in ice flow models?, J. Geophys. Res. Earth Surf., 122, 2269–2282, 2017.
 - Larour, E., Schiermeier, J., Rignot, E., Seroussi, H., Morlighem, M., and Paden, J.: Sensitivity Analysis of Pine Island Glacier ice flow using ISSM and DAKOTA, J. Geophys. Res., 117, F02009, 1–16, 2012.
- Larour, E., Utke, J., Csatho, B., Schenk, A., Seroussi, H., Morlighem, M., Rignot, E., Schlegel, N., and Khazendar, A.: Inferred basal friction and surface mass balance of the Northeast Greenland Ice Stream using data assimilation of ICESat (Ice Cloud and land Elevation Satellite) surface altimetry and ISSM (Ice Sheet System Model), Cryosphere, 8, 2335–2351, 2014.
 - MacAyeal, D. R.: Large-scale ice flow over a viscous basal sediment: Theory and application to Ice Stream B, Antarctica, J. Geophys. Res., 94, 4071–4087, 1989.
- Masutani, M., Woollen, J. S., Lord, S. J., Emmitt, G. D., Kleespies, T. J., Wood, S. A., Greco, S., Sun, H., Terry, J., Kapoor, V., et al.: Observing system simulation experiments at the National Centers for Environmental Prediction, J. Geophys. Res. Atmos., 115, 2010.
 - Morlighem, M., Seroussi, H., Larour, E., and Rignot, E.: Inversion of basal friction in Antarctica using exact and incomplete adjoints of a higher-order model, J. Geophys. Res., 118, 1746–1753, 2013.
- Morzfeld, M. and Hodyss, D.: A theory for why even simple covariance localization is so useful in ensemble data assimilation, Mon. Weather Rev., 151, 717–736, 2023.
 - Mouginot, J., Rignot, E., Scheuchl, B., and Millan, R.: Comprehensive Annual Ice Sheet Velocity Mapping Using Landsat-8, Sentinel-1, and RADARSAT-2 Data, Remote Sens., 9, 2017.



510



- Müller, S., Schüler, L., Zech, A., and Heße, F.: GSTools v1. 3: a toolbox for geostatistical modelling in Python, Geosci. Model Dev., 15, 3161–3182, 2022.
- Nowicki, S. and Seroussi, H.: Projections of future sea level contributions from the Greenland and Antarctic Ice Sheets: Challenges beyond dynamical ice sheet modeling, Oceanography, 31, 2018.
 - Nowicki, S. M. J., Payne, A. J., Larour, E., Seroussi, H., Goelzer, H., Lipscomb, W. H., Gregory, J., Abe-Ouchi, A., and Shepherd, A.: Ice Sheet Model Intercomparison Project (ISMIP6) contribution to CMIP6, Geosci. Model Dev., 9, 4521–4545, 2016.
- Rodriguez-Morales, F., Gogineni, S., Leuschen, C. J., Paden, J. D., Li, J., Lewis, C. C., Panzer, B., Gomez-Garcia Alvestegui, D., Patel,
 A., Byers, K., Crowe, R., Player, K., Hale, R. D., Arnold, E. J., Smith, L., Gifford, C. M., Braaten, D., and Panton, C.: Advanced
 Multifrequency Radar Instrumentation for Polar Research, IEEE Trans. Geosc. and Rem. Sens., 52, 2824–2842, 2014.
 - Seroussi, H., Morlighem, M., Rignot, E., Larour, E., Aubry, D., Ben Dhia, H., and Kristensen, S. S.: Ice flux divergence anomalies on 79north Glacier, Greenland, Geophys. Res. Lett., 38, 1–5, 2011.
- Seroussi, H., Morlighem, M., Larour, E., Rignot, E., and Khazendar, A.: Hydrostatic grounding line parameterization in ice sheet models, Cryosphere, 8, 2075–2087, 2014.
 - Seroussi, H., Nowicki, S., Simon, E., Abe-Ouchi, A., Albrecht, T., Brondex, J., Cornford, S., Dumas, C., Gillet-Chaulet, F., Goelzer, H., Golledge, N. R., Gregory, J. M., Greve, R., Hoffman, M. J., Humbert, A., Huybrechts, P., Kleiner, T., Larour, E., Leguy, G., Lipscomb, W. H., Lowry, D., Mengel, M., Morlighem, M., Pattyn, F., Payne, A. J., Pollard, D., Price, S. F., Quiquet, A., Reerink, T. J., Reese, R., Rodehacke, C. B., Schlegel, N.-J., Shepherd, A., Sun, S., Sutter, J., Van Breedam, J., van de Wal, R. S. W., Winkelmann, R., and Zhang, T.: initMIP-Antarctica: an ice sheet model initialization experiment of ISMIP6, Cryosphere, 13, 1441–1471, 2019.
 - Seroussi, H., Nowicki, S., Payne, A. J., Goelzer, H., Lipscomb, W. H., Abe-Ouchi, A., Agosta, C., Albrecht, T., Asay-Davis, X., Barthel, A., Calov, R., Cullather, R., Dumas, C., Galton-Fenzi, B. K., Gladstone, R., Golledge, N. R., Gregory, J. M., Greve, R., Hattermann, T., Hoffman, M. J., Humbert, A., Huybrechts, P., Jourdain, N. C., Kleiner, T., Larour, E., Leguy, G. R., Lowry, D. P., Little, C. M., Morlighem, M., Pattyn, F., Pelle, T., Price, S. F., Quiquet, A., Reese, R., Schlegel, N.-J., Shepherd, A., Simon, E., Smith, R. S., Straneo, F., Sun, S.,
- 515 Trusel, L. D., Van Breedam, J., van de Wal, R. S. W., Winkelmann, R., Zhao, C., Zhang, T., and Zwinger, T.: ISMIP6 Antarctica: a multi-model ensemble of the Antarctic ice sheet evolution over the 21st century, The Cryosphere, 14, 3033–3070, 2020.
 - Smith, B., Fricker, H. A., Holschuh, N., Gardner, A. S., Adusumilli, S., Brunt, K. M., Csatho, B., Harbeck, K., Huth, A., Neumann, T., et al.: Land ice height-retrieval algorithm for NASA's ICESat-2 photon-counting laser altimeter, Remote Sens. Environ., 233, 111 352, 2019.
- Smith, B., Dickinson, S., Jelley, B. P., Neumann, T. A., Hancock, D., Lee, J., and Harbeck, K.: ATLAS/ICESat-2 L3B Slope-Corrected Land

 Ice Height Time Series, Version 6, https://doi.org/10.5067/ATLAS/ATL11.006, 2023.
 - Smith, B., Sutterley, T., Dickinson, S., Jelley, B. P., Felikson, D., Neumann, T. A., Fricker, H. A., Gardner, A. S., Padman, L., Markus, T., Kurtz, N., Bhardwaj, S., Hancock, D., and Lee, J.: ATLAS/ICESat-2 L3B Gridded Antarctic and Arctic Land Ice Height Change, Version 4, https://doi.org/10.5067/ATLAS/ATL15.004, 2024.
- Tippett, M. K., Anderson, J. L., Bishop, C. H., Hamill, T. M., and Whitaker, J. S.: Ensemble square root filters, Mon. Weather Rev., 131, 1485–1490, 2003.
 - Zhang, Y.-F., Bitz, C. M., Anderson, J. L., Collins, N., Hendricks, J., Hoar, T., Raeder, K., and Massonnet, F.: Insights on sea ice data assimilation from perfect model observing system simulation experiments, J. Clim., 31, 5911–5926, 2018.